Optical Fiber Technology 19 (2013) 583–586

Contents lists available at ScienceDirect

Optical Fiber Technology

www.elsevier.com/locate/yofte

# A simple fiber-optic humidity sensor based on extrinsic Fabry–Perot cavity constructed by cellulose acetate butyrate film

Wei Xu [a,c], Wo-Bin Huang [a], Xu-Guang Huang [a,*], Chang-yuan Yu [b,c]

[a] Laboratory of Nanophotonic Functional Materials and Devices, School for Information and Optoelectronic Science and Engineering, South China Normal University, Guangzhou 510006, China
[b] Department of Electrical and Computer Engineering, National University of Singapore, Singapore 117583, Singapore
[c] Center of Advanced Microelectronic Devices, National University of Singapore Research Institute, Suzhou 215000, China

ARTICLE INFO

*Article history:*
Received 8 April 2013
Revised 26 July 2013
Available online 5 October 2013

*Keywords:*
Fiber optic
Fabry–Perot
Relative humidity
Thin-film

ABSTRACT

A fiber-optic relative humidity sensor with an extrinsic micro Fabry–Perot cavity constructed with a thin layer of cellulose acetate butyrate coated on a fiber end is presented. Its operational principle is based on the relative-humidity-dependent wavelength shift of the interference fringes formed by Fresnel reflections from both interfaces of the thin film. Both the experimental and theoretical analyses are investigated in detail. The experimental data for relative humidity ranging from 8.8% to 88.1% are measured in the both humidification and dehumidification processes, which fits the linear equation very well with a value of $R^2 = 0.9946$. As observed, it shows a high sensitivity of 0.307 nm/%RH with a high resolution of 0.06%. The time-dependent response of the sensor is estimated. The long term stability of the sensor is also addressed with high precision of ±0.03% over 100 min. The proposed relative humidity sensor has a simple, solid, and compact structure.



## 1. Introduction

Humidity is one of the most important physical quantities in the field of physics. It plays a significant role in diverse range of applications, including structure monitoring, agriculture, pharmacy, meteorology, etc. In various industries and environments, the relative humidity (RH) is usually used to describe the humidity and is defined as the ratio of the actual vapor density of water to the saturation vapor density at a specific temperature. A common way to relate the amount of the water vapor is to take the water vapor pressure, i.e., $RH = p/p_s \times 100\%$ [1], where $p$ is the partial water vapor pressure, and $p_s$ is the saturation water vapor pressure. Conventional RH sensors include types of capacitive and resistive sensors. A resistive one has non-linear response, while a capacitive one has linear response in a wide range. However, both of them are prone to be influenced by electromagnetic fields. Though other RH sensors such as mechanical (hair) hygrometers, wet and dry bulb psychrometers are immune to electromagnetic, they suffer from low resolution, read-on mode or complex operation, etc [2–4].

So far, fiber-optic humidity sensors have attracted plenty of research interests due to their particular advantages, including immunity to electromagnetic field, small size, corrosion resistant, remote and real-time sensing [5]. Fiber-optic RH sensors with characteristics of optical absorption [6,7], scattering [8,9] and fluorescence [10,11] are effective ways to monitor the RH. Such as, polymethylmethacrylate (PMMA) film with phenol red doped and MgO film with nano-size particles can be used to sense the RH owing to their RH-dependent absorption mechanism. As for evanescent-wave scattering-based RH sensors, including types of bent and taper, materials coated on the fiber perform as a cladding, so the intensity of the transmitted light varies with the different RH environments. However, these intensity-dependent sensors are influenced by the variation of their light sources. Luminescence lifetime-based methods monitor the RH through measuring the fluorescence time, which may avoid light intensity variations, but lack long-term stability owing to the dyes in the host material bleaching and leaching [4].

Polymers with hygroscopic swelling characteristic inducing expansion or refractive index (RI) change can be used to monitor the RH as well. Utilizing grating techniques, Liu et al. [12] proposed a sensor using long period grating (LPG) coated with hydrogel providing the sensitivity of 0.2 nm/%RH and the accuracy of RH, while Yeo et al. [13] proposed a polymer-coated fiber Bragg grating (FBG) sensor for RH measure with the maxim sensitivity of ~5.6 pm/%RH. However, grating-based sensors have weak points of complex fabrication process and somewhat friability. Interferometry-based RH sensors have been reported a lot because of being insensitive to fluctuation of the light source and high measure sensitivity. Wu et al. [14] utilized a microfiber knot resonator sensor with PMMA

* Corresponding author.
*E-mail address:* huangxg@scnu.edu.cn (X.-G. Huang).

1068-5200/$ - see front matter © 2013 Elsevier Inc. All rights reserved.
http://dx.doi.org/10.1016/j.yofte.2013.09.005

coated achieving a sensitivity of 8.8 pm/%RH. Gu et al. [4] utilized the fiber modal interferometer achieving a resolution of 0.78% RH and a sensitivity of 84.3 pm/%RH, and Chen et al. [15] utilized the Fabry–Perot (FP) technique achieving a sensitivity of 0.13 nm/%RH and a RH uncertain of ±1.68. All of them still suffer complex fabrication process or relatively low sensitivity.

In this letter, a simple fiber-optic RH sensor with higher sensitivity of 0.307 nm/%RH and high resolution of 0.06% is proposed. It is mainly based on an extrinsic micro FP cavity constructed by a thin film of cellulose acetate butyrate (CAB) coated on the fiber end. It is based on FP interference fringes from a FP cavity formed by the two interfaces of the film and the relation between its wavelength shift and the RH. Both the theoretical analysis and experimental setup of the method are discussed in detail. The feasibility of the presented method is verified by the measurement of different RH environments ranging from 8.8% to 88.1%. The whole system consists of non-bulk fiber optic components without any optical alignment. It is of compact and solid structure, simple operation and fabrication, insensitive to fluctuation of the light source, real-time monitoring, higher sensitivity and resolution, which has a potential in practical use and industrialization.

## 2. Principle of operation

The structure of the sensing head is sketched in Fig. 1(a), which shows a thin film at the end of the single-mode fiber with a vertical interface. The module structure contains both hydrophilic and hydrophobic groups, which is shown in Fig. 1(a). The CAB film layer was formed with spin-coating technique on the end of a PC fiber adaptor. It was rotated at appropriate speed in order to spread the material. The higher the angular speed of the spinning, the thinner the film can be made. We spun the fiber at the speed around 200 rpm for ~50 s to evenly spread the CAB at room temperature. A FP cavity is formed by fiber–thin-film interface and thin-film–air interface, labeled 1 and 2 with a length of $L$. As shown in Fig. 3, one can read out the wavelength difference between two adjacent troughs to be approximately 16.8 nm. Through the equation of $\Delta\lambda \approx \frac{\lambda_0^2}{2nL}$, assuming that $n$ equals 1.4558 [16] and $\lambda_0$ equals 1550 nm, one can estimate the thickness $L \approx 50$ μm. The sensing head is immersed in a stable RH environment where the RH is to be measured. $n_f$, $n_{air}$ and $n$ are denoted as the refractive indices of the fiber core, the air and the CAB film, respectively. $r_1$ and $r_2$

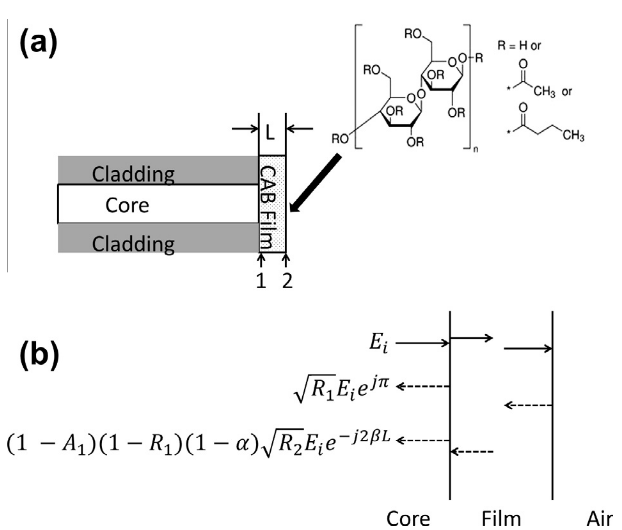


**Fig. 1.** (a) Structure of the sensing head and the molecular structure of CAB and (b) the field amplitude at the reflection interfaces, $R_1$, $R_2$ respectively represent the reflection coefficients from interface 1 and 2.

are respectively the amplitude reflection coefficients at surface 1 and 2, which can be described as follows according to Fresnel formula [15]:

$$r_1 = \frac{n_f - n}{n_f + n}, \quad r_2 = \frac{n - n_{air}}{n + n_{air}} \tag{1}$$

As shown in Fig. 1(b), the $E_i$ represents the input field of the incident light. The reflected fields from two surfaces compose the total reflected field $E_r$, which can be written as

$$\begin{aligned} E_r &= r_1E_ie^{j\pi} + \sum_{i=1}^{\infty}(1-A_1)(1-r_1^2)(1-\alpha)^i r_1^{i-1} r_2^i E_i \times e^{-j2\beta L*i} \\ &= r_1E_ie^{j\pi} + \frac{(1-A_1)(1-r_1^2)(1-\alpha)E_ir_2e^{-j2\beta L}}{1-(1-\alpha)r_1r_2e^{-j2\beta L}} \\ &= \frac{(K+Q)e^{-j2\beta L} - P + Qe^{j2\beta L}}{M}E_i \end{aligned} \tag{2}$$

where $K = (1-A_1)(1-r_1^2)(1-\alpha)r_2$, $P = (1-A_1)(1-r_1^2)(1-\alpha)^2r_1r_2^2 + (1-\alpha)^2r_1^3r_2^2 + r_1$, $Q = (1-\alpha)r_1^2r_2$, $M = 1 + (1-\alpha)^2r_1^2r_2^2 - 2(1-\alpha)r_1r_2\cos(4\pi Ln/\lambda)$, $A_1$ is the transmission loss factor owing to the imperfection (e.g., roughness) of the surface 1, $\beta$ is the propagation constant in the film media, and $\alpha$ is the loss factor in the cavity. In Eq. (2), only the first-order reflection fields from the two surfaces are taken into account, while the high-order reflections is neglected owing to the low reflection coefficients. From Eq. (2), a normalized reflection spectrum $R_{FP}(\lambda)$ is obtained as follows:

$$\begin{aligned} R_{FP}(\lambda) &= |E_r/E_i|^2 \\ &= \frac{(K+Q)^2 + Q^2 + P^2 + 2Q(K+Q)\cos(8\pi Ln/\lambda) - 2P(K+2Q)\cos(4\pi Ln/\lambda)}{M^2} \end{aligned} \tag{3}$$

If we neglect the second order and higher order reflection terms from two interfaces, i.e., $P \approx r_1$, $Q \approx 0$, $M \approx 1$. Therefore, Eq. (3) can be simplified into follows:

$$R_{FP}(\lambda) = r_1^2 + K^2 - 2r_1K\cos(4\pi Ln/\lambda) \tag{4}$$

This equation demonstrates the interference pattern of the reflected light from the sensing head with a FP cavity. As shown in Eq. (4), there exist maximum and minimum values according to different wavelengths of $\lambda$. $\lambda_{\min}$, denoted as the wavelength where the value of $R_{FP}(\lambda_{\min})$ drops to a minimum, agrees with the following equation given by

$$4\pi Ln/\lambda_{\min} = 2m\pi \tag{5}$$

where $m$ is the $m$'th-order interference fringe. From Eq. (5), one could obtain

$$\lambda_{\min} = 2Ln/m \tag{6}$$

When the ambient RH changes, the length of the thin film and the RI will change owing to water absorption. Therefore, if the ambient RH changes, $\lambda_{\min}$ will be given by

$$\lambda_{\min} = \frac{2}{m}(L + \alpha_l \cdot \Delta RH)(n + \alpha_n \cdot \Delta RH) \tag{7}$$

where $\alpha_l = \partial L/\partial RH$ is moisture expansion coefficient and $\alpha_n = \partial n/\partial RH$ is RH-optic coefficient. One could see that the wavelength of $\lambda_{\min}$ will change due to the variation of $L$ and $n$ of the thin film. Therefore, the measurement of RH will be translated into the measurement and calculation of a wavelength shift.

The experiment setup is illustrated in Fig. 2. It consists of a flattened broad band source (BBS) whose wavelength ranging from 1525 nm to 1565 nm, an optical circulator, an optical spectrum analyzer (OSA, AQ6370) whose resolution is 0.02 nm and a fiber sensing end with a thin film of CAB. The sensing end is immersed into a bottle where different RH environments are generated